Bulgarian Chemical Communications, Volume 49, Special Edition K2, (pp. 195 – 199) 2017

Large eddy simulation of multiphase flow in button - type micro channels

Zh. He, J. Liu, X.-Y. Sun *, X. Gu

College of Aerospace and Civil Engineering, Harbin Engineering University, Harbin 150001 China

Received August 18, 2017; Accepted December 18, 2017

The reduction of the micro channel scale creates surface tension, wettability cannot be ignored, the capillary action and the friction between the fluid and the wall also play an important role, which makes difficult the direct observation. In this paper, various structure-micro channels with cross-sectional area of 200 μm × 200 μm were taken as the research object. Numerical simulation based on Smagorinsky model and VOF model (for dealing with multiphase flow interface problems) was used as research method to study the mixing effect of fluids in the micro channel. The results showed that the distance between the two button nodes, the node diameter, the distribution position, and the channel entrance angle have a certain effect on the mixing effect in the micro channel.

Keywords: Micro channels, LES, VOF, Mixed effect, Numerical simulation

AIMS AND BACKGROUND

The flow characteristics of the fluid in a micro channel are very different from those in a general pipeline. Micro channels are widely used in the fields of electronics, aerospace and biotechnology because of their fast reaction rate and simple structure. With the development of computer technology, numerical simulation has been used to study micro channel problems and obvious results have been achieved. The numerical simulation can be a simple and economical method to respond to some phenomena in the micro channel, which is of great significance for the study of the mixing effect in the micro channel.

Yagmur *et al.* [1] used the large eddy simulation (LES) turbulence model in ANSYS-Fluent software to simulate the flow around a triangular column. The separation point of the flow and the Carmen vortex formed in the wake region were simulated. This shows that the large eddy simulation can well simulate the flow phenomenon.

Zhang *et al.* [2] used the dynamic model of the LES model to simulate the 60 ° inclined jet with a bottom impact, and compared the simulation results of the dynamic model and the k-ε model. When simulated by the k-ε model, the change of the reaction concentration is stable, and no local accumulation at the impact point was observed. The dynamic model could be used to observe the phenomenon, which indicated that the simulation results were more accurate.

Hu *et al*. [3] carried out large eddy simulation of the axial flow of a cylinder with different inclination angles. The LES turbulence model was used and the results showed that a turbulence vortex was formed on the rear side of the cylinder, which improved the efficiency of the washing. The larger the inclination angle, the better was the cleaning effect.

EXPERIMENTAL

Theory

The large eddy simulation (LES) builds on the turbulence statistical theory and the understanding of the Quasi-ordered structure overcomes the defects of the traditional turbulence model in time averaged processing and universality, which core is the simulation of sub-grid (small-scale movement) Reynolds stress [2]. At present, the commonly used sub-grid scale model is the Smagorinsky model, dynamic model, structure function model and so on.

Mass fraction equation and momentum equation were used to describe the VOF model [4]:

$$\frac{\alpha_q^{n+1}\rho_q^{n+1}-\alpha_q^n\ \rho_q^n}{\Delta t}V+\sum_f(\rho_q^{n+1}U_f^{n+1}\alpha_{q,f}^{n+1})=\left[S_{\alpha_q}+\sum_{p=1}^{n}\dot{m}_{pq}-\dot{m}_{qp}\right] \quad (1)$$

where:

n+1 = index for current time step;
n = index for previous time step;
α_q^{n+1}= cell value of volume fraction at time step n+1;
α_q^n = cell value of volume fraction at time step n;
$\alpha_{q,f}^{n+1}$ = face value of the q^{th} volume fraction at time step n+1;
U_f^{n+1} = volume flux through the face at time step n+1;
V = cell volume;

$$\frac{\partial}{\partial t}(\rho\vec{v})+\nabla\cdot(\rho\vec{v}\vec{v})=-\nabla\rho+\nabla\cdot[\mu(\nabla\vec{v}+\nabla\vec{v}^T)]+\rho\vec{g}+\vec{F} \quad (2)$$

In this paper, a button-type micro channel with a cross-sectional area of 200 μm × 200 μm was taken as the research object. Channel length is 6 mm, lengths of three entry sections are 0.9 mm, distance between the first button-type node to the inlet 3 is 2 mm, basic phase is water, second phase is air. Water flows from inlet 1 and inlet 2 into the channel, air flows from inlet 3 into the channel, the flow rate is

To whom all correspondence should be sent:
E-mail: sunxiaoyu520634@163.com

0.1m/s, the three inlets are velocity inlets, the outlet is a pressure outlet, the pressure is the standard atmospheric pressure. Using pressure-velocity couple algorithm, the pressure difference program selected PRESTO! algorithm, the time dispersion method is Bounded second order implicit format, and the momentum equation discrete mode is Bounded central differencing format, the time step is 0.0001 s, Courant number, sub-relaxation iterative factor and other parameters were selected according to the stability and convergence of calculation. The calculation model is shown in Fig. 1.

Fig. 1. Calculation model

As the size of the micro channel and the macro pipe varies widely, resulting in a large difference in boundary conditions, according to the different Knudsen number, several intervals can be distinguished [5]:

1）$\mathrm{Kn} \to 0$ （$\mathrm{Re} = 0$）

Ignores the diffusion term, satisfies the Euler equation;

2) $\mathrm{Kn} \ll 10^{-3}$

Satisfies the N-S equation, suitable for non-slip boundary condition;

3）$10^{-3} \ll \mathrm{Kn} \ll 10^{-1}$

Satisfies the N-S equation, not suitable for non-slip boundary condition;

4）$10^{-1} \ll \mathrm{Kn} \ll 10$

Transition zone;

5）$\mathrm{Kn} > 10$

Belongs to a free molecular flow.

Where Kn=l/L，l is the molecular free path, L is the characteristic size of the micro device. In the standard state, the effective diameter of the air molecule is 3.5×10^{-10} m, the average molecular weight is 29. Using the above formula the calculated average free path is $= 6.9 \times 10^{-8}$m. In this paper, the characteristic size of the model is L=2×10^{-4}m, and Kn=1.75×10^{-6} - much less than 10^{-3}, so it is suitable for non-slip boundary conditions.

The channels are segmented using a regular hexahedral mesh. In order to eliminate the effect of grid density on the simulation results, a grid independence test is performed. The change in the section air fraction with the number of grids is shown in Fig. 2.

It can be seen from Fig. 2 that when the number of grids is greater than 1200000, the section air fraction almost no longer changes, the number of grids increases from 1200000 to 2000000, the section air fraction is reduced by 1.32%. It can be assumed that the numerical simulation of the number of grids is 1200000 as a grid independent solution.

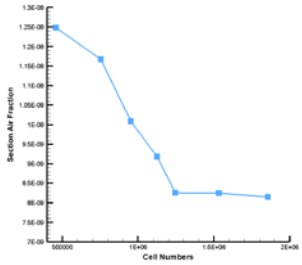

Fig. 2. Grid-independent validation

To study the effect of two button-type spacing and nodal diameter on the mixing effect in the channel, two button-type spacing of 500μm, 800μm, 1200μm, and node diameters of 200μm and 400μm, respectively, were taken. The water distribution cloud of the vertical section at 0.0028 m from the outlet and the cross section at 0.000175 m from the upper surface of the channel are shown in Figs. 3 and 4, respectively.

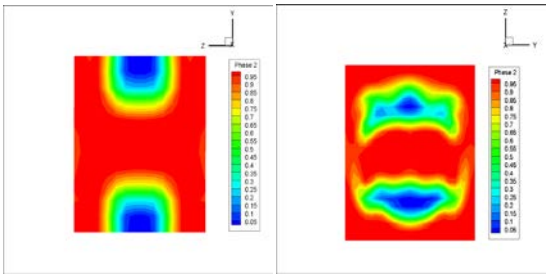

(a) 500 200 (b)800 200

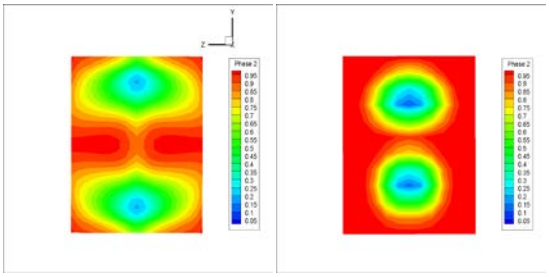

(c)1200 200 (d)500 400

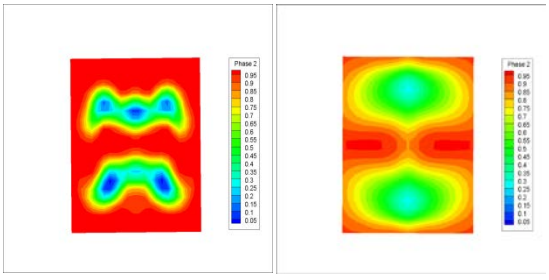

(e)800 400 (f)1200 400

Fig. 3. The water distribution cloud of the vertical section

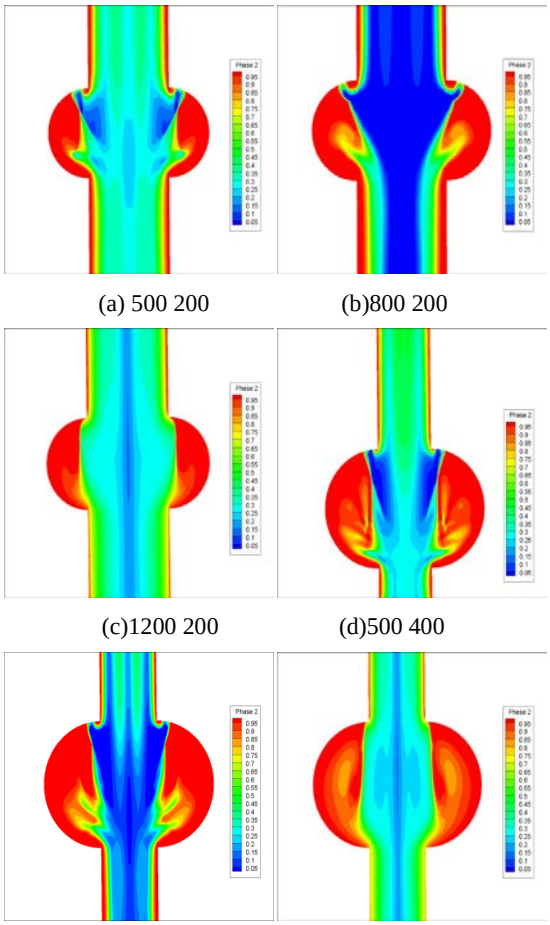

(a) 500 200 (b)800 200

(c)1200 200 (d)500 400

(e)800 400 (f)1200 400

Fig. 4. The water distribution cloud of the cross section

In order to study the effect of the nodal distribution position on the mixing effect in the channel when the channel entrance angle is 90 °, the nodes were placed on the same plane as the channel entrance, perpendicular to the channel entrance plane. The water distribution cloud of the vertical cross section at a distance from the outlet section of 0.0028 m is shown in Fig. 5.

To investigate the effect of the nodal distribution position on the mixing effect in the channel when the channel entrance angle is 45 °, the nodes were placed on the same plane as the channel entrance perpendicular to the channel entrance plane. The water distribution cloud of the vertical cross section at distance from the outlet section of 0.0028 m is shown in Fig. 6.

To investigate the effect of channel entrance angle on the mixing effect in the channel, the inlet angle was taken as 45° or 90°. The water distribution cloud of the vertical section at 0.0028 m from the outlet section and the cross section at 0.000175 m from the upper surface of the channel are shown in Figs. 7 and 8.

In order to compare the accuracy of the distribution of the cloud, the section air fraction of the vertical section at 0.0028 m from the outlet section was calculated. The results are shown in Table 1.

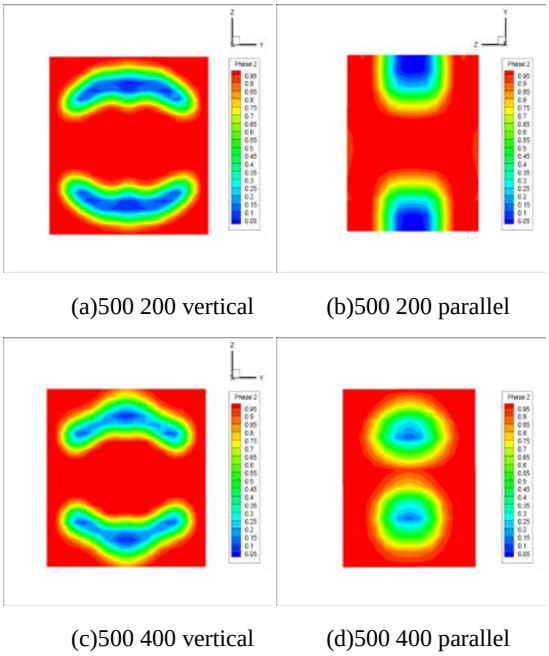

(a)500 200 vertical (b)500 200 parallel

(c)500 400 vertical (d)500 400 parallel

Fig. 5. The water distribution cloud of the vertical section

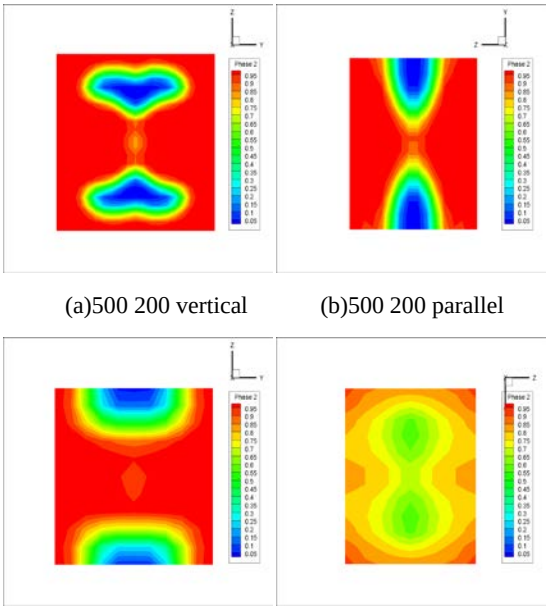

(a)500 200 vertical (b)500 200 parallel

(c)500 400 vertical (d)500 400 parallel

Fig. 6. The water distribution cloud of the vertical section

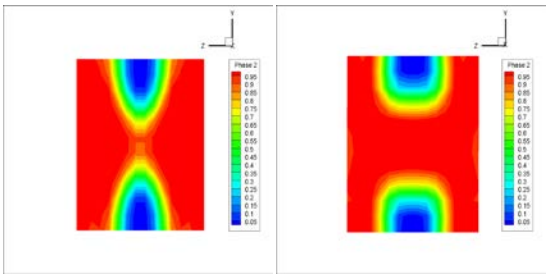

（a）500 200 45°　　（b）500 200 90°

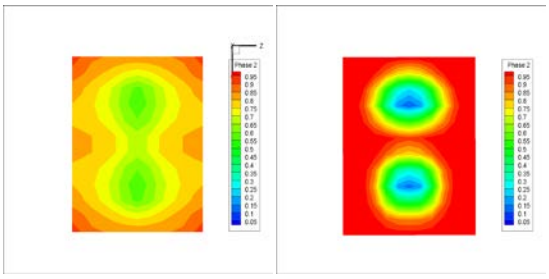

（c）500 400 45°　　（d）500 400 90°

Fig. 7. The water distribution cloud of the vertical section

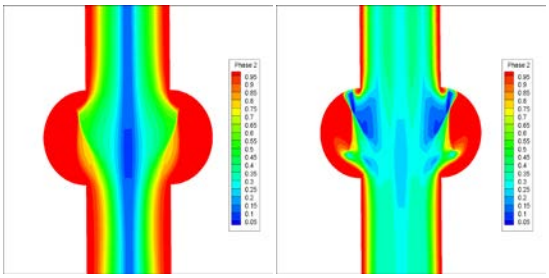

(a)　500 200 45°　　(b) 500 200 90°

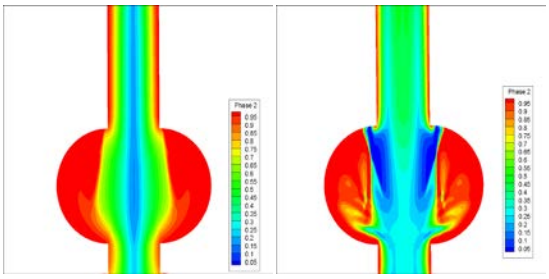

(c) 500 400 45°　　(d)　500 400 90°

Fig. 8. The water distribution cloud of the cross section

Table1. Section air fraction

Nodal spacing (μm)	Nodal diameter (μm)	Position distribution of the nodes	Entrance angle (°)	Air phase area (m^2)	Distance from the outlet section	Time	Air fraction
12000	200	parallel	90	1.1282280E-08	0.0028m	0.05s	28.21%
800	200	parallel	90	8.9983620E-09			22.50%
500	200	parallel	90	8.2554070E-09			20.64%
500	400	parallel	90	7.3176700E-09			18.29%
800	400	parallel	90	7.8148170E-09			19.54%
1200	400	parallel	90	1.0916560E-08			27.29%
500	200	Vertical	90	9.0497850E-09			22.62%
500	400	Vertical	90	8.6280130E-09			21.57%
500	200	parallel	45	7.9874200E-09			19.97%
500	200	Vertical	45	7.7125440E-09			19.28%
500	400	parallel	45	9.9487690E-09			24.87%
500	400	Vertical	45	8.4233990E-09			21.06%

RESULTS AND DISCUSSION

It can be seen from Fig. 3 that when the nodal diameter is 200μm, with the larger nodal spacing, air distribution is more and more uniform. The data in Table 1 show that the section air fraction increases from 20.64% to 28.21% when the nodal spacing increases from 500μm to 1200μm. This is so because as the nodal spacing becomes larger, the decrease in the amount of air remaining in the channel leads to a greater increase in the section air fraction. The air distribution is more uniform when the nodal spacing is 500μm, the section air fraction decreases from 20.64% to 18.29% when the nodal diameter increases from 200μm to 400μm, The air distribution is more concentrated. It can be seen from Fig. 4 that at constant nodal diameter, as the space of the nodal becomes larger, the vortices at the node are significantly reduced, the mixing effect at the nodule decreases and the air fraction becomes larger (see Figure 3). When the space is constant and the diameter of the node changes from 200μm to 400μm, the vortices at the node increase, indicating that the mixing effect in the micro channel is better when the nodal diameter is 400μm. The above description shows that when the node diameter is constant, with the increase in nodal spacing the air fraction of the section becomes larger. When the space is constant, with the increase in nodal spacing the air fraction of the section becomes smaller. The gas distribution is more concentrated.

It can be seen from Fig. 5 that if the channel entrance angle is 90 ° and the nodal diameter is 200 μm, when the button structure changes from vertical

distribution to parallel distribution, the section air fraction decreases from 22.62% to 20.64%. When the nodal diameter is 400 μm, the above air fraction is also reduced from 21.57% to 18.29%. Note that when the button type node and the channel entrance are on the same plane, the air distribution is more concentrated with a better mixing effect.

It can be seen from Fig. 6 that at a channel entrance angle of 45 ° and nodal diameter of 200 μm, when the button structure changes from vertical distribution to parallel distribution, the section air fraction increases from 19.28% to 19.97%. When the nodal diameter is 400 μm, the above air fraction also increases from 21.06% to 24.87%. Note that when the button type node is vertical to the channel entrance plane, the air distribution is more concentrated with a better mixing effect.

It can be seen from Fig. 7 that for a nodal spacing of 500μm and nodal diameter of 200μm, when the inlet angle is from 45 ° to 90 ° and the section air fraction from 19.97% to 20.64%, the change is not obvious. For a nodal spacing of 500μm and nodal diameter of 400μm, when the inlet angle is from 45 ° to 90 ° and the section air fraction is from 24.87% to 18.29%，Fig. 8 shows that when the entrance angle is 90 °, the vortices at the button-type node increase and the air stays at the nodules, resulting in smaller air fraction. It is shown that the effect of the angle change on the section air fraction is small when the diameter of the node is small, and the effect of the angle change on the section air fraction increases as the diameter of the node becomes larger. For a channel entrance angle of 45 °, when the node diameter is from 200μm to 400μm, the section air fraction increases from 19.97% to 20.64%. For a channel entrance angle of 90 °, when the node diameter is from 200μm to 400μm, the section air fraction increases from 24.87% to 18.29%. Note that for an inlet angle of 45°, if the diameter of the node is increased, the air fraction also increases. For an inlet angle of 90 °, if the diameter of the node is increased, the air fraction decreases.

CONCLUSIONS

When the inlet angle is 90 °, with the increase in the node space, the section air fraction becomes larger and the gas distribution more uniform. With the increase in the node diameter, the section air fraction becomes smaller and the gas distribution more focused.

When the inlet angle is 45 °, the mixing effect of the vertical distribution is better than that of the parallel distribution. The larger the node diameter, the worse is the mixing effect. When the inlet angle is 90 °, the parallel distribution of the button type node is better than the vertical distribution; the greater the diameter of the node, the better is the mixing effect.

As the diameter of the nodal increases, the effect of the angle change on the section air fraction increases.

Acknowledgements: *This work was financially supported by the National Natural Science Foundation of China（No. 11602066）and the China Postdoctoral Science Foundation On the 56th bath of surface founds the project (2014M561327) and the National Science Foundation of Heilongjiang Province of China (QC2015058 and 42400621-1-15047), the Foundation Research Funds for the Central Universities.*

REFERENCES

1. S. Yagmur, S. Dogan, M. H. Aksoy, I. Goktepeli, M. Ozgoren, *Flow Measurement and Instrumentation*, **55**, 23 (2017).
2. Sh Zhang, A W.-K. Law, M. Jiang, *Journal of Hydro-environment Research*, **15**, 54 (2017).
3. G. Hu, K.T. Tse, K.C.S. Kwok, Y. Zhang, **146,** 172 (2015).
4. S.S. Lafmejani, A.C. Olesen, S.K. Kær, *International Journal of Hydrogen Energy*, **42** (26), 16333 (2017).
5. D.M. Bond, V. Wheatley, M. Goldsworthy, *International Journal of Heat and Mass Transfer*, **76,** 1 (2014).